

ARTICLE

Received 16 Apr 2012 | Accepted 14 Aug 2012 | Published 18 Sep 2012

DOI: 10.1038/ncomms2067

The elusive Heisenberg limit in quantum-enhanced metrology

Rafał Demkowicz-Dobrzański¹, Jan Kołodyński¹ & Mădălin Guță²

Quantum precision enhancement is of fundamental importance for the development of advanced metrological optical experiments, such as gravitational wave detection and frequency calibration with atomic clocks. Precision in these experiments is strongly limited by the $1/\sqrt{N}$ shot noise factor with N being the number of probes (photons, atoms) employed in the experiment. Quantum theory provides tools to overcome the bound by using entangled probes. In an idealized scenario this gives rise to the Heisenberg scaling of precision $1/N$. Here we show that when decoherence is taken into account, the maximal possible quantum enhancement in the asymptotic limit of infinite N amounts generically to a constant factor rather than quadratic improvement. We provide efficient and intuitive tools for deriving the bounds based on the geometry of quantum channels and semi-definite programming. We apply these tools to derive bounds for models of decoherence relevant for metrological applications including: depolarization, dephasing, spontaneous emission and photon loss.

¹ Faculty of Physics, University of Warsaw, ul. Hoża 69, PL-00-681 Warszawa, Poland. ² School of Mathematical Sciences, University of Nottingham, University Park, NG7 2RD Nottingham, UK. Correspondence and requests for materials should be addressed to R.D.-D. (email: demko@fuw.edu.pl).

Quantum-enhanced metrology aims to exploit quantum features of atoms and light such as entanglement, for measuring physical quantities with precision going beyond the classical limit^{1–4}. A prominent example is that of an optical interferometer, where interference of photons at the output port carries information on the relative optical path difference between the interferometer arms. When standard laser light is used, the observed results are compatible with the claim that ‘each photon interferes only with itself’⁵ and the whole process may be regarded as sensing with N independent probes (photons). Parameter estimation with N independent probes yields the $1/\sqrt{N}$ ‘standard scaling’ (SS) of precision⁶. Entangling the probes however, can in principle offer a quadratic enhancement in precision, that is, the $1/N$ or ‘Heisenberg scaling’ (HS)^{7–11}. Such strategies have been experimentally realized in optical interferometry^{12–16} with exciting applications in the quest for the first direct detection of gravitational waves^{17,18}. Moreover, the same quantum enhancement principle can be utilized in atomic spectroscopy^{19,20} where the spin-squeezed states have been employed for improving frequency calibration precision^{21–24}. Alternative approaches to beat the SS without resorting to quantum entanglement include multiple-pass^{25,26} and non-linear metrology^{27,28}.

Unfortunately, both the theory^{29–35} and experiments^{36,37} confirmed the fragility of the above schemes when noise sources such as decoherence are considered, and it has been rigorously shown for particular models that asymptotically with respect to N , even infinitesimally small noise turns HS into SS, so that the quantum gain amounts to a constant factor improvement^{38–40}.

In this paper, we develop two methods that allow us to extend these partial results to a broad class of decoherence models, and in particular to obtain fundamental bounds on quantum enhancement for the most relevant models encountered in the quantum metrology literature. The two approaches complement each other in terms of provided intuition and power. The first method elaborates on the idea of ‘classical simulation’ (CS)⁴¹ and provides a bound based solely on the geometry of the space of quantum channels (SQC). When applicable, it gives an excellent intuition as to why the HS is lost in the presence of decoherence, but fails to yield useful bounds for some relevant decoherence models. The second method is based on the ‘channel extension’ (CE) strategy⁴² and requires the optimization over different Kraus representation of a quantum channel. However, unlike the earlier work⁴⁰, which involved making an educated guess about the appropriate class of Kraus representations, our bound can be cast into an explicit semi-definite optimization problem, which is easy to solve even for complex models. The power of the method is demonstrated by obtaining new bounds for depolarization and spontaneous emission models, and re-deriving asymptotic bounds for dephasing and lossy interferometer with unprecedented simplicity.

Results

Bounds on precision in quantum-enhanced metrology. The typical quantum metrology scenario is depicted in Fig. 1a. An ensemble of N quantum systems undergo in parallel the same transformation Λ_φ , which depends on an unknown physical parameter φ . The output state is measured and the outcome is used to compute an estimate $\tilde{\varphi}$ of the parameter φ as summarized below

$$\varphi \rightarrow \Lambda_\varphi^{\otimes N} [\rho^N] \rightarrow \tilde{\varphi}. \quad (1)$$

The task is to find the optimal (possibly highly entangled) input state ρ^N and the most effective measurement strategy to minimize the estimation error $\Delta\varphi_N$. Note that since the decoherence process is assumed to act independently on each of the probes, the global channel is described by the tensor product $\Lambda_\varphi^{\otimes N}$.

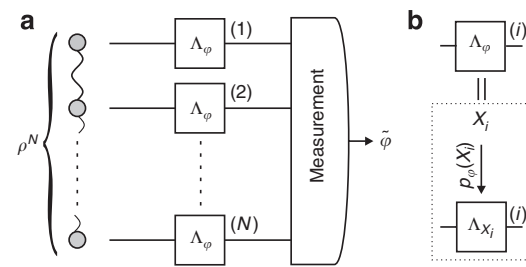


Figure 1 | Quantum metrology and the CS idea. (a) General scheme for quantum-enhanced metrology. N -probe quantum state fed into N parallel channels is sensing an unknown channel parameter φ . An estimator $\tilde{\varphi}$ is inferred from a measurement result on the output state. (b) CS of a quantum channel. The channel Λ_φ is interpreted as a mixture of other channels Λ_{X_i} , where the dependence on φ is moved into the mixing probabilities $p_\varphi(X)$.

We pursue the estimation problem by restricting our attention to estimators, which are unbiased in the neighbourhood of some fixed parameter value, for which the quantum Cramér–Rao bound (CRB) holds

$$\Delta\varphi_N \geq \frac{1}{\sqrt{F_Q[\Lambda_\varphi^{\otimes N}[\rho^N]]}}, \quad (2)$$

where F_Q is the quantum Fisher information (QFI)⁹. Maximization of QFI over input states ρ^N sets the limit on the achievable quantum-enhanced precision:

$$\Delta\varphi_N \geq \frac{1}{\sqrt{F_N}}, \quad F_N = \max_{\rho^N} F_Q[\Lambda_\varphi^{\otimes N}[\rho^N]]. \quad (3)$$

The states that maximize the QFI and yield the HS for decoherence-free unitary channels are typically highly entangled: the GHZ state in the case of atomic spectroscopy⁴³, and the N00N state in the case of optical interferometry⁴⁴. In the presence of decoherence, the optimal input states do not have an intuitive form and the maximization of the QFI (with rising N) becomes hard even numerically^{20,29,30}.

The typical behaviour of the estimation uncertainty in the presence of decoherence is depicted in the log–log scale in Fig. 2, showing that asymptotically in N the quantum gain amounts to a constant factor improvement over the standard $1/\sqrt{N}$ scaling achievable with independent probes. The key result of this paper is to provide a method for a general and simple calculation of this constant factor improvement.

Classical simulation. To understand the idea of CS, we need to think of quantum channels in a geometrical way⁴⁵. A quantum channel is a completely positive, trace-preserving map acting on density matrices. The space of all such transformations is convex: if Λ, Λ' are two channels, then $p\Lambda + (1-p)\Lambda'$ can be realised by randomly applying Λ or Λ' with probabilities p and $1-p$. The channels that cannot be decomposed into a convex combination of different channels (for example, the unitary transformations) are called ‘extremal’. Note that while all interior points of the SQC are ‘non-extremal’, the boundary contains both the extremal as well as some non-extremal channels.

We say that the family Λ_φ is ‘classically simulated’⁴¹ if each channel is written as a classical mixture of the form

$$\Lambda_\varphi[\rho] = \int dx p_\varphi(x) \Lambda_x[\rho], \quad (4)$$

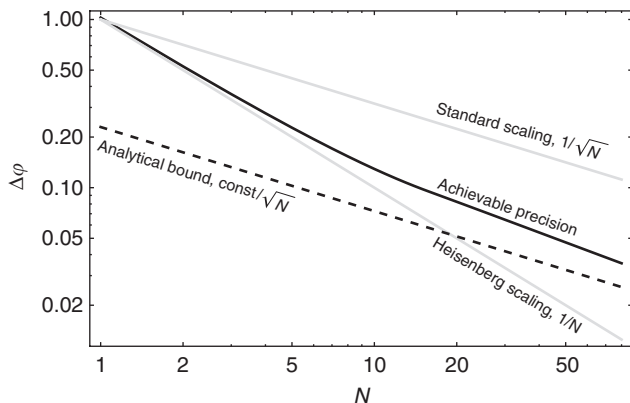


Figure 2 | Estimation precision in presence of decoherence. Log-log plot of a generic dependence of quantum-enhanced parameter estimation uncertainty in the presence of decoherence as a function of the number of probes used. While for small number of probes the curve for achievable precision follows the Heisenberg scaling, it asymptotically flattens to approach const/\sqrt{N} dependence. The ‘const’ represents the quantum enhancement factor. The exemplary data corresponds to the case of phase estimation using N photons in a Mach-Zehnder interferometer with 5% losses in both arms.

where the unknown parameter enters only through the probability distribution p_φ of a random variable X that indicates which channel to pick from the set $\{\Lambda_x\}$ (Fig. 1b). If X_1, \dots, X_N are the independent hidden random variables used to generate the parallel channels, we can rewrite the estimation problem as

$$\varphi \rightarrow \{X_i\}_{i=1}^N \rightarrow \otimes_{i=1}^N \Lambda_{X_i} [\rho^N] \rightarrow \tilde{\varphi}. \quad (5)$$

Since conditionally on the values of X_i the output state does not carry any information about φ , the estimation precision in the above scenario is at most equal to that of the classical problem of estimating φ given N independent samples from the distribution p_φ

$$\varphi \rightarrow \{X_i\}_{i=1}^N \rightarrow \tilde{\varphi}. \quad (6)$$

Hence, using the classical CRB⁴⁶, we obtain a lower bound on the uncertainty of the original problem equation (1)

$$\Delta\varphi_N \geq \frac{1}{\sqrt{N} F_{\text{cl}}[p_\varphi]}, \quad F_{\text{cl}} = \int dx \frac{[\partial_\varphi p_\varphi(x)]^2}{p_\varphi(x)}, \quad (7)$$

where F_{cl} is the classical Fisher information; see Methods for an alternative derivation.

Provided that $p_\varphi(x)$ satisfies regularity conditions required in the derivation of CRB⁴⁶, the SS of precision follows immediately. Moreover, any particular CS yields an explicit SS bound on precision. If many CSs are possible, we obtain the tightest SS bound for $\Delta\varphi_N$ by choosing the ‘worst’ decomposition yielding minimal $F_{\text{cl}}[p_\varphi]$, as shown below. On the other hand, HS is possible only when the above conditions are not satisfied. This happens, for example, in the decoherence-free case where Λ_φ are unitary channels, which are extremal points of the SQC and the only admissible p_φ in equation (4) is the irregular Dirac delta distribution being zero on all channels except Λ_φ .

The QFI at a given φ_0 depends only on the output state and its first derivative at φ_0 . This implies that any family of channels $\tilde{\Lambda}_\varphi$,

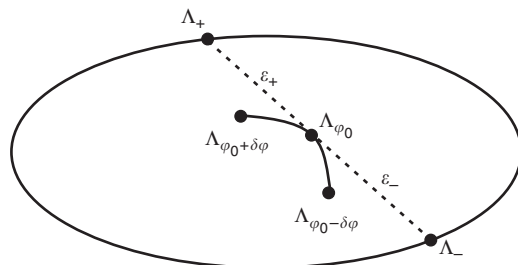


Figure 3 | Local classical stimulation. Schematic representation of a local classical stimulation (CS) of a channel Λ_φ at φ_0 that lies inside the convex set of quantum channels (solid oval). The optimal CS has to be valid only in the neighbourhood of Λ_{φ_0} along the curve $\{\Lambda_\varphi\}_{\varphi_0 \pm \delta\varphi}$ (solid arched line) and corresponds to a binary mixture of channels Λ_\pm , which rest on the tangent (dashed) line at the two outermost points. Then, the precision of estimation can be lower bounded just using the distances ε_\pm .

which ‘locally coincides’ with the original one, that is,

$$\tilde{\Lambda}_{\varphi_0}[\rho] = \Lambda_{\varphi_0}[\rho], \quad \partial_\varphi \tilde{\Lambda}_{\varphi}[\rho]|_{\varphi_0} = \partial_\varphi \Lambda_\varphi[\rho]|_{\varphi_0}, \quad (8)$$

achieves the same maximum QFI in equation (3). It is therefore enough to consider the ‘local classical simulations’, that is, any mixtures reproducing the channel and its first derivative at given φ_0 . As proven in Supplementary Methods, the CS with the smallest F_{cl} can be constructed using two channels, $\{\Lambda_+, \Lambda_-\}$, which lie on the tangent line to the ‘channel trajectory’ at the two outermost points situated on the boundary of the set of channels (Fig. 3). The local CS around φ_0 reads explicitly

$$\tilde{\Lambda}_\varphi[\rho] = p_\varphi^+ \Lambda_+[\rho] + p_\varphi^- \Lambda_-[\rho], \quad (9)$$

with

$$\Lambda_\pm[\rho] = \Lambda_{\varphi_0}[\rho] \pm \varepsilon_\pm \partial_\varphi \Lambda_\varphi[\rho]|_{\varphi_0}, \quad p_\varphi^\pm = \frac{\varepsilon_\mp \pm (\varphi - \varphi_0)}{\varepsilon_+ + \varepsilon_-}.$$

Making use of equation (7) applied to the binary probability distribution p_φ^\pm , we obtain

$$\Delta\varphi_N \geq \sqrt{\frac{\varepsilon_+ \varepsilon_-}{N}}. \quad (10)$$

To calculate the above bound it suffices to find the ‘distances’ ε_\pm of the channel from the boundary measured along the tangent line. For extremal channels, $\varepsilon_\pm = 0$ and the bound is not useful. For non-extremal channels, the above construction will yield a finite F_{cl} provided that $\varepsilon_\pm > 0$, that is, Λ_{φ_0} can be decomposed into a mixture of channels lying on the tangent. Channels that have this additional property will be called ‘ φ -non-extremal’. They obey the standard precision scaling, and include all full-rank channels (that is, channels lying in the interior of the SQC)^{41,42}. An explicit method for calculating ε_\pm and hence the bound for a general quantum channel is described in the Methods.

Channel extension. Even though the CS method is very general, there are interesting examples of ‘ φ -extremal’ decoherence models for which CS does not apply. In this case, one can resort to the more powerful but less intuitive CE method.

The action of the quantum channel Λ_φ can be described via its Kraus representation⁴⁷:

$$\Lambda_\varphi[\rho] = \sum_i K_i(\varphi) \rho K_i^\dagger(\varphi), \quad (11)$$

with Kraus operators satisfying $\sum_i K_i(\varphi)^\dagger K_i(\varphi) = \mathbb{1}$. Although this representation is not unique, different sets of linearly independent Kraus operators are related by unitary transformations

$$\tilde{K}_i(\varphi) = \sum_j u_{ij}(\varphi) K_j(\varphi), \quad (12)$$

where $u(\varphi)$ is a unitary matrix possibly depending on φ .

An equivalent definition of the QFI has been proposed^{40,42}

$$F_Q[\Lambda_\varphi[\rho]] = \min_{|\Psi_\varphi\rangle} F_Q(|\Psi_\varphi\rangle), \quad (13)$$

where the minimization is performed over all φ differentiable purifications of the output state

$$\Lambda_\varphi[\rho] = \text{Tr}_E \{ |\Psi_\varphi\rangle\langle\Psi_\varphi| \}. \quad (14)$$

For pure input state, different purifications correspond to different equivalent Kraus representations of the channel, as in equation (12). For many quantum metrological models⁴⁰, one can make an educated guess of a purification and derive excellent input-independent analytical bounds providing the correct asymptotic scaling of precision. Nevertheless, the method may be cumbersome especially when the channel description involves many Kraus operators.

A simpler bound can be derived by exploiting the intuitive observation that allowing the channel to act in a trivial way on an extended space, can only improve the precision of estimation, that is,

$$\max_\rho F_Q[\Lambda_\varphi[\rho]] \leq \max_{\rho_{\text{ext}}} F_Q[\Lambda_\varphi \otimes \mathbb{I}[\rho_{\text{ext}}]]. \quad (15)$$

This leads to an upper bound on \mathcal{F}_N , which goes around the input state optimization, yielding⁴²:

$$\mathcal{F}_N \leq 4 \min_{\tilde{K}} \left\{ N \|\alpha_{\tilde{K}}\| + N(N-1) \|\beta_{\tilde{K}}\|^2 \right\} \quad (16)$$

where $\|\cdot\|$ denotes the operator norm, the minimization is performed over all equivalent Kraus representations of Λ_φ , and

$$\alpha_{\tilde{K}} = \sum_i \dot{\tilde{K}}_i^\dagger(\varphi) \dot{\tilde{K}}_i(\varphi), \quad \beta_{\tilde{K}} = i \sum_i \dot{\tilde{K}}_i^\dagger(\varphi) \tilde{K}_i(\varphi), \quad (17)$$

where $\dot{\tilde{K}}_i(\varphi) = \partial_\varphi \tilde{K}_i(\varphi)$. For any given $\varphi = \varphi_0$, equation (16) involves only \tilde{K}_i and its first derivatives at φ_0 . Moreover, the bound is insensitive to changing the Kraus representations with a φ -independent u . Therefore, it is enough to parameterize equivalent Kraus representations in equation (12) with a hermitian matrix h , which is generator of $u(\varphi) = \exp[-ih(\varphi - \varphi_0)]$. This reduces the optimization problem equation (16) to a minimization over h .

As the SS of precision holds when \mathcal{F}_N scales linearly with N , the bound equation (16) implies that a sufficient condition for SS is to find h for which $\beta_{\tilde{K}} = 0$, or equivalently⁴²:

$$\sum_{i,j} h_{ij} K_i^\dagger K_j = i \sum_q \dot{K}_q^\dagger K_q. \quad (18)$$

Here we go a step further and show that in this case we can obtain a quantitative SS bound

$$\mathcal{F}_N \leq 4N \min_h \|\alpha_{\tilde{K}}\|, \quad (19)$$

where the minimization runs over h satisfying equation (18), and can be formulated as a semi-definite program, as described in the Methods section.

Moreover, it turns out that the bound resulting from finding the global minimum in equation (19) is at least as tight as the one derived using the CS method based on equation (7) (see Supplementary Methods) proving superiority of the CE over the CS method.

Examples. All examples of channels presented below are of the form $\Lambda_\varphi[\rho] = \Lambda[U_\varphi \rho U_\varphi^\dagger]$, that is, a concatenation of a unitary rotation encoding the estimated parameter φ and an φ -independent decoherence process. Consequently, $K_i(\varphi) = K_i U_\varphi$, where $K_i(\varphi)$, K_i are the Kraus operators of Λ_φ and Λ , respectively. The most relevant models in quantum-enhanced metrology belong to this class, but the methods presented may be applied to more general models as well.

In what follows, we adopt the standard notation where $\mathbb{1}$ is the 2×2 identity matrix and $\{\sigma_i\}_{i=1}^3$ are the Pauli operators. We focus on two-level probe systems (qubits) sensing a phase shift modelled using a unitary $U(\varphi) = \exp[i(\sigma_3 \varphi)/2]$ —rotation of the Bloch ball around the z axis. In the case of atomic clocks' frequency calibration $\varphi = \delta\omega \cdot t$ with $\delta\omega$ being the detuning between the frequency of the atomic transition and the frequency of driving field, while t is the time of evolution. Even though in practice the parameter to be estimated is $\delta\omega$, we will consider that to be φ , to have a unified notation for atomic and optical models. In the case of a two-mode optical interferometer, $U(\varphi)$ is the operator acting on a single photon state, accounting for the accumulated relative phase shift φ between the two arms of the interferometer.

We apply the methods to four decoherence processes encountered in quantum-enhanced metrology: two-level atom depolarization, dephasing, spontaneous emission and the photon loss inside the interferometer. These examples will provide us with the full picture of the applicability of the methods discussed in the paper, as they cover all distinct cases from the point of view of the geometry of SQC.

Depolarization. Two-level atom depolarization describes an isotropic loss of coherence and may be visualized by a uniform Bloch ball shrinking (Fig. 4a) where $0 \leq \eta < 1$ is the final Bloch ball radius. Its description involves four Kraus operators

$$K_0 = \sqrt{\frac{1+3\eta}{4}} \mathbb{1}, \quad \left\{ K_i = \sqrt{\frac{1-\eta}{4}} \sigma_i \right\}_{i=1\dots 3} \quad (20)$$

which makes it an example of a channel lying in the interior of the SQC. Using CS method, we infer the SS of precision and calculate the 'distances' from the boundary of the SQC $\varepsilon_\pm = \sqrt{(1-\eta)(1+3\eta)/(2\eta)}$ (see Methods) resulting in the bound presented in Table 1. Applying

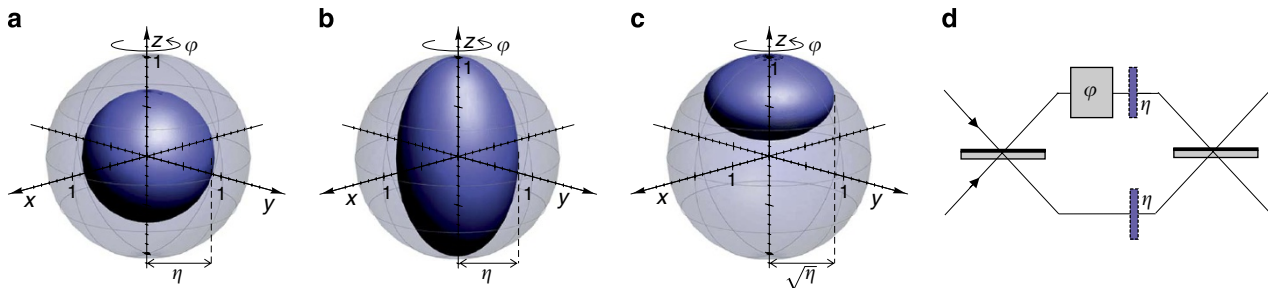


Figure 4 | Graphical representation of decoherence models. Two-level atom decoherence processes are illustrated with a corresponding shrinking of the Bloch ball (blue) for the cases of: (a) depolarization, (b) dephasing and (c) spontaneous emission. The estimated parameter φ represents the angle of rotation about the z axis, whereas η specifies the strength of decoherence and effectively the size of shrinkage in the x - y plane. In the example (d) of the lossy interferometer, φ corresponds to the additional phase acquired by photons travelling in the upper arm and η stands for the power transmission coefficient in each of the arms.

Table 1 | Precision bounds of the most relevant models in quantum-enhanced metrology.

Channel considered	Classical simulation	Channel extension
Depolarisation	$\sqrt{(1-\eta)(1+3\eta)/4\eta^2}$	$\sqrt{(1-\eta)(1+2\eta)/2\eta^2}$
Dephasing	$\sqrt{1-\eta^2/\eta}$	$\sqrt{1-\eta^2/\eta}$
Spontaneous emission	NA	$(1/2)\sqrt{1-\eta/\eta}$
Lossy interferometer	NA	$\sqrt{1-\eta/\eta}$

NA, not available.

The bounds are derived using the two methods discussed in the paper. All the bounds are of the form $\Delta\varphi_N \geq (\text{const}/\sqrt{N})$, where constant factors are given in the table. Classical simulation method does not provide bounds for spontaneous emission and lossy interferometer, as these channels are φ -extremal. For the dephasing model, it surprisingly yields an equally tight bound as the more powerful channel extension method.

the CE method, it is possible to further improve the bound and the analytical result of the semi-definite optimization is also shown in Table 1. The only non-zero elements of the corresponding optimal h are $h_{03} = h_{30} = \sqrt{(1-\eta)(1+3\eta)}/c$ and $h_{12} = -h_{21} = -i(1+\eta)/c$ where $c = 2(1-\eta)(1+2\eta)$. To our best knowledge, the bound has not been derived before.

Dephasing. Dephasing is a decoherence model of two-level atoms subject to fluctuating external magnetic/laser fields. In graphical representation, it corresponds to shrinking of the Bloch ball in x , y directions with z direction intact (Fig. 4b). The canonical Kraus operators read⁴⁷

$$K_0 = \sqrt{\frac{1+\eta}{2}} \mathbb{1}, \quad K_1 = \sqrt{\frac{1-\eta}{2}} \sigma_3, \quad (21)$$

where $0 \leq \eta < 1$ is the dephasing parameter. As it involves only two Kraus operators, it is not a full-rank channel and lies on the boundary of the SQC. It is, however, a non-extremal and more importantly φ -non-extremal channel allowing for the CS construction with $\varepsilon_{\pm} = \sqrt{1-\eta^2}/\eta$ (see Methods), yielding the bound given in Table 1.

Most importantly, the above bound, is exactly the same as the one derived by Escher *et al.*⁴⁰ or by the CE method, where the minimum in equation (19) corresponds to $h = \sigma_1/\left(2\sqrt{1-\eta^2}\right)$. This proves that despite its simplicity the CS method may sometimes lead to

bounds that are equally tight as the ones derived with much more advanced methods even for channels lying on the boundary of the SQC.

Spontaneous emission. The well-known two-level atom spontaneous emission model is described by the Kraus operators

$$K_0 = \begin{pmatrix} 1 & 0 \\ 0 & \sqrt{\eta} \end{pmatrix}, \quad K_1 = \begin{pmatrix} 0 & \sqrt{1-\eta} \\ 0 & 0 \end{pmatrix} \quad (22)$$

with $0 \leq \eta < 1$. Interestingly, for all η this channel is extremal⁴⁸, which means that the CS is not applicable. Nevertheless, the CE method of equation (19) can be easily employed.

Substituting $K_i(\varphi)$ into equation (18), we find that the generator h is fixed to $h = \frac{1}{2(1-\eta)}(\sigma_z - \eta\mathbb{1})$. Consequently, there is no need for minimization over h and from equation (19) we automatically obtain an SS bound listed in Table 1, which to our knowledge has not been reported in the literature before.

Lossy interferometer. To model ‘loss’ in an optical interferometer, a third orthogonal state at the output,—vacuum—resulting from a loss of a photon, needs to be introduced. The decoherence channel on a single probe (single photon) is a map from a two- to a three-dimensional system:

$$K_0 = \begin{pmatrix} 0 & 0 \\ 0 & 0 \\ 0 & \sqrt{1-\eta} \end{pmatrix}, \quad K_1 = \begin{pmatrix} 0 & 0 \\ 0 & 0 \\ \sqrt{1-\eta} & 0 \end{pmatrix}, \quad K_2 = \begin{pmatrix} \sqrt{\eta} & 0 \\ 0 & \sqrt{\eta} \\ 0 & 0 \end{pmatrix}, \quad (23)$$

where η is the power transmission coefficient for the light travelling through each of the two arms. Although the corresponding channel Λ_φ is non-extremal, it is unfortunately φ -extremal and CS cannot be used. Still, CE method can be easily applied. The optimal bound (see Table 1) corresponds to h with non-zero elements $h_{00} = -h_{11} = \frac{1}{2(1-\eta)}$. This bound is asymptotically equally tight to the best bounds known in the literature^{38–40}, proving again that CE method despite its simplicity is able to provide powerful results in a straightforward manner.

In optical interferometric applications, it is common to use states of light with an unbounded number of photons, such as coherent or squeezed states^{49–53}. At a first glance, it is not obvious that the model considered in the paper covers these situations. Formally speaking, the bound we have derived applies to input states with a total number of photons fixed to N . Notice, however, that in every

optical experiment what is measured in the end are photon numbers. If all phase reference beams are taken into account, we can regard quantum states of light as incoherent mixtures of states occupying different total photon number sectors^{53,54}. From the point of view of metrology, the QFI is then bounded from above by the weighted sum of QFIs for each of these sectors³⁰. Within each sector we can easily apply our bound and, as the bound is linear in N , the effective bound will simply correspond to replacing N with \bar{N} —the mean number of photons in all relevant beams used in the experiment—and as such can be automatically applied to experiments involving coherent and squeezed light.

To demonstrate the practical relevance of the bound, it is instructive to compare its predictions with the actual quantum enhancement observed recently in the GEO600 gravitational wave detector¹⁷. Although a detailed theoretical analysis of the set-up from the perspective of the derived bounds is still underway, by reducing the essential features of the set-up to a simple Mach-Zehnder interferometer, we can already give a preliminary estimate on how far is the actual experiment from the optimal performance. For the reported overall optical transmission $\eta = 0.62$, the theoretically predicted maximal quantum enhancement amounts to a $\sqrt{1-\eta} = 0.62$ factor reduction in estimation uncertainty compared with the classical $1/\sqrt{\eta\bar{N}}$ limit. The reported experimentally observed reduction was a factor of 0.67, which is an indication that the experiment operates close to the fundamental quantum limit and any significant improvement is possible only if the optical loss is further reduced.

Discussion

Assessing the impact of decoherence on the maximum possible quantum enhancement is a crucial element in developing quantum techniques for metrological applications. The tools developed here allow for a direct calculation of bounds on the precision enhancement for arbitrary parameter estimation model where the decoherence process acts independently on each of the probes and may be represented with a finite number of Kraus operators. The CE method is more powerful and for the most relevant metrological models yields in the asymptotic limit of large number of probes the tightest bounds known in the literature. Yet the CS method, which may fail to provide equally tight bounds, provides an intuitive geometric insight into the absence of asymptotic HS in the presence of decoherence. From the derived bounds, it is clear that if the HS was to be preserved for large number of probes N the level of decoherence would have to decrease with increasing N roughly as $(1-\eta) \approx 1/N$. This gives an estimate on the regime in which the quantum enhancement is quadratic as compared with the regime of constant factor improvement. This is clearly seen in Fig. 2 where this transition appears around $N \approx 1/(1-\eta) = 20$ for $\eta = 0.95$. As in most metrology applications N is larger by several order of magnitude, we expect that the SS scaling provides a reliable bound for the optimal estimation precision.

An important question that was not addressed here is the saturation of the bounds. The CS method does not provide tight bounds in general. As for the CE method, we are not able to prove that the bounds we have derived are saturable in the asymptotic limit. We should stress however, that these are lower bounds on estimation uncertainties and an upper bound can always be found by choosing a particular estimation method. Therefore, if a certain strategy performs close to the derived bound, we can certify that it is not far from reaching the fundamental quantum limit, as illustrated by the results of the GEO600 experiment.

Even though the minimization over purification method⁴⁰ yields in principle a tight bound, in practice there is no effective algorithm to find a global minimum, and the only way to convince oneself that one has achieved the global minimum is again to show that the

theoretical lower bound on estimation uncertainty coincides with the performance of a particular estimation strategy.

The methods discussed were focused on deriving useful bounds in the asymptotic regime of a large number of probes. Still, the bounds are valid (though weaker) for any value of N . We leave it for a future work to improve the bounds for finite N , which seems to be possible by using the CE method and relaxing the $\beta_{\tilde{K}} = 0$ constraint.

Methods

Proof of the CS bound. To simplify the reasoning, let us focus on the CSs that are constructed using discrete sets of quantum channels, $\{\Lambda_i\}$. Then, the considered channel's action of equation (4) can be rewritten as a φ -independent map acting on a larger input space⁴¹

$$\Lambda_{\varphi}[\rho] = \sum_i p_{\varphi,i} \Lambda_i[\rho] = \Phi[\rho \otimes \sigma_{\varphi}], \quad (24)$$

where $\sigma_{\varphi} = \sum_i p_{\varphi,i} |e_i\rangle\langle e_i|$ represents a diagonal state in some basis, in which Φ is defined via $\Phi[\rho] = \sum_i (\Lambda_i \otimes E_i)[\rho]$ with $E_i[\sigma] = \langle e_i | \sigma | e_i \rangle$. To prove equation (7), we write the QFI for the N parallel use of the channel and bound it from above, that is

$$\begin{aligned} F_Q[\Lambda_{\varphi}^{\otimes N}[\rho]] &= F_Q[\Phi^{\otimes N}[\rho \otimes \sigma_{\varphi}^{\otimes N}]] \\ &\leq F_Q[\rho \otimes \sigma_{\varphi}^{\otimes N}] = F_Q[\sigma_{\varphi}^{\otimes N}] = N F_Q[\sigma_{\varphi}] = N F_{\text{cl}}[p_{\varphi}], \end{aligned} \quad (25)$$

exploiting the monotonicity of the QFI under any parameter-independent quantum map⁵⁵, here $\Phi^{\otimes N}$.

Calculation of the CS bound. The geometry of the space of channels and more specifically the φ -extremality are best viewed by using the Choi-Jamiolkowski isomorphism^{56,57}. Given a quantum channel $\Lambda : \mathcal{L}(\mathcal{H}_{\text{in}}) \mapsto \mathcal{L}(\mathcal{H}_{\text{out}})$ acting from the space of density matrices on \mathcal{H}_{in} to density matrices on \mathcal{H}_{out} , one defines $P_{\Lambda} = \Lambda \otimes \mathbb{I} |\Psi\rangle\langle\Psi|$, where $|\Psi\rangle = \sum_{i=1}^{d_{\text{in}} d_{\text{in}}} |i\rangle\otimes|i\rangle$ is a maximally entangled state in $\mathcal{H}_{\text{in}} \otimes \mathcal{H}_{\text{in}}$. Λ is a physical channel (that is, trace preserving, completely positive map) if P_{Λ} is a positive semi-definite operator, satisfying $\text{Tr}_{\mathcal{H}_{\text{out}}} \{P_{\Lambda}\} = \mathbb{I}$. If $\{K_i\}_i$ are the Kraus operators of the Λ channel, we can write explicitly $P_{\Lambda} = \sum_i |K_i\rangle\langle K_i|$, where $|K_i\rangle = K_i \otimes \mathbb{I} |\Psi\rangle$.

We can now say that the channel Λ_{φ} is φ -non-extremal, if it is possible to find a non-zero ε , for which $P_{\Lambda_{\varphi}} \pm \varepsilon \partial_{\varphi} P_{\Lambda_{\varphi}} \geq 0$. See Supplementary Methods for an alternative formulation of the φ -non-extremality condition and its relation to the well-known non-extremality condition due to Choi⁵⁷. In practice, if we want to make most out of the bound in equation (10), we need to find the maximum values of ε_{\pm} , for which $P_{\Lambda_{\varphi}} \pm \varepsilon_{\pm} \partial_{\varphi} P_{\Lambda_{\varphi}}$ are still positive semi-definite operators. This is a simple eigenvalue problem and therefore the bound can be obtained immediately.

Taking the dephasing model as an example, the Choi-Jamiolkowski isomorphism of the corresponding Λ_{φ} channel $P_{\Lambda_{\varphi}} = \sum_{i=1}^2 |K_i U_{\varphi}\rangle\langle K_i U_{\varphi}|$ has a simple form:

$$P_{\Lambda_{\varphi}} = \begin{pmatrix} 1 & 0 & 0 & \eta e^{i\varphi} \\ 0 & 0 & 0 & 0 \\ 0 & 0 & 0 & 0 \\ \eta e^{-i\varphi} & 0 & 0 & 1 \end{pmatrix}. \quad (26)$$

It is easy to check that $P_{\Lambda_{\varphi}} + \varepsilon \partial_{\varphi} P_{\Lambda_{\varphi}} \geq 0$ provided $|\varepsilon| \leq \sqrt{1-\eta^2}/\eta$, hence using equation (10) we arrive at the bound given in Table 1.

CE method as a semi-definite program. Here we show that the minimization problem in equation (19) can be formulated as a simple semi-definite program. Let the channel Λ_{φ} be a map from a d_1 - to a d_2 -dimensional Hilbert spaces with Kraus representation involving k linear independent Kraus operators ($d_2 \times d_1$ matrices). Consider the following block matrix:

$$A = \begin{pmatrix} \sqrt{\varepsilon} \mathbb{I}_{d_1} & \dot{K}_0^{\dagger} & \dot{K}_1^{\dagger} & \dots & \dot{K}_{k-1}^{\dagger} \\ \dot{K}_0 & \sqrt{\varepsilon} \mathbb{I}_{d_2} & 0 & \dots & 0 \\ \dot{K}_1 & 0 & \sqrt{\varepsilon} \mathbb{I}_{d_2} & \dots & 0 \\ \vdots & \vdots & \vdots & \ddots & \vdots \\ \dot{K}_{k-1} & 0 & 0 & \dots & \sqrt{\varepsilon} \mathbb{I}_{d_2} \end{pmatrix}, \quad (27)$$

where $\mathbb{1}$ is a $d \times d$ identity matrix. Positive semi-definiteness of the matrix A is equivalent to the condition

$$\alpha_{\tilde{K}} = \sum_i \tilde{K}_i^\dagger \tilde{K}_i \leq t \mathbb{1}_{d_1}. \quad (28)$$

Minimizing the operator norm $\|\alpha_{\tilde{K}}\|$ is thus equivalent to minimizing t subject to $A \geq 0$. Taking into account equation (18), the problem takes the form:

$$\min_h t, \text{ subject to: } A \geq 0, \sum_{ij} h_{ij} K_i^\dagger K_j = i \sum_q \tilde{K}_q^\dagger K_q. \quad (29)$$

Since $\tilde{K}_i = \tilde{K}_i - i \sum_j h_{ij} K_j$ the matrix A is linear in h and the problem is thus a semi-definite program with the resulting minimal t being the minimal operator norm $\|\alpha_{\tilde{K}}\|$. For the purpose of this paper, we have implemented the program using the CVX package for Matlab⁵⁸.

References

1. Giovannetti, V., Lloyd, S. & Maccone, L. Advances in quantum metrology. *Nat. Photon.* **5**, 222–229 (2011).
2. Maccone, L. & Giovannetti, V. Quantum metrology: beauty and the noisy beast. *Nat. Phys.* **7**, 376–377 (2011).
3. Paris, M. G. A. Quantum estimation for quantum technology. *Int. J. Quant. Inf.* **7**, 125–137 (2009).
4. Banaszek, K., Demkowicz-Dobrzanski, R. & Walmsley, I. A. Quantum states made to measure. *Nat. Photon.* **3**, 673–676 (2009).
5. Dirac, P. A. M. *The Principles of Quantum Mechanics* (Oxford University Press, 1958).
6. Kahn, J. & Gută, M. Local asymptotic normality for finite dimensional quantum systems. *Commun. Math. Phys.* **289**, 597–652 (2009).
7. Giovannetti, V., Lloyd, S. & Maccone, L. Quantum-enhanced measurements: beating the standard quantum limit. *Science* **306**, 1330–1336 (2004).
8. Giovannetti, V., Lloyd, S. & Maccone, L. Quantum metrology. *Phys. Rev. Lett.* **96**, 010401 (2006).
9. Braunstein, S. L. & Caves, C. M. Statistical distance and the geometry of quantum states. *Phys. Rev. Lett.* **72**, 3439–3443 (1994).
10. Berry, D. W. & Wiseman, H. M. Optimal states and almost optimal adaptive measurements for quantum interferometry. *Phys. Rev. Lett.* **85**, 5098–5101 (2000).
11. Zwierz, M., Prez-Delgado, C. A. & Kok, P. General optimality of the heisenberg limit for quantum metrology. *Phys. Rev. Lett.* **105**, 180402 (2010).
12. Mitchell, M. W., Lundein, J. S. & Steinberg, A. M. Super-resolving phase measurements with a multi-photon entangled state. *Nature* **429**, 161–164 (2004).
13. Eisenberg, H. S., Hodelin, J. F., Khoury, G. & Bouwmeester, D. Multiphoton path entanglement by nonlocal bunching. *Phys. Rev. Lett.* **94**, 090502 (2005).
14. Nagata, T., Okamoto, R., O'Brien, J. L., Sasaki, K. & Takeuchi, S. Beating the standard quantum limit with four entangled photons. *Science* **316**, 726–729 (2007).
15. Resch, K. J. *et al.* Time-reversal and super-resolving phase measurements. *Phys. Rev. Lett.* **98**, 223601 (2007).
16. Higgins, B. L. *et al.* Demonstrating heisenberg-limited unambiguous phase estimation without adaptive measurements. *New J. Phys.* **11**, 073023 (2009).
17. LIGO Collaboration.. A gravitational wave observatory operating beyond the quantum shot-noise limit. *Nat. Phys.* **7**, 962–965 (2011).
18. Goda, K. *et al.* A quantum-enhanced prototype gravitational-wave detector. *Nat. Phys.* **4**, 472–476 (2008).
19. Wineland, D. J., Itano, W. M., Bollinger, J. J. & Moore, F. L. Spin squeezing and reduced quantum noise in spectroscopy. *Phys. Rev. A* **46**, R6797–R6800 (1992).
20. Huelga, S. F. *et al.* Improvement of frequency standards with quantum entanglement. *Phys. Rev. Lett.* **79**, 3865–3868 (1997).
21. Meyer, V. *et al.* Experimental demonstration of entanglement-enhanced rotation angle estimation using trapped ions. *Phys. Rev. Lett.* **86**, 5870–5873 (2001).
22. Leibfried, D. *et al.* Toward heisenberg-limited spectroscopy with multiparticle entangled states. *Science* **304**, 1476–1478 (2004).
23. Wasilewski, W. *et al.* Quantum noise limited and entanglement-assisted magnetometry. *Phys. Rev. Lett.* **104**, 133601 (2010).
24. Koschorreck, M., Napolitano, M., Dubost, B. & Mitchell, M. W. Sub-projection-noise sensitivity in broadband atomic magnetometry. *Phys. Rev. Lett.* **104**, 093602 (2010).
25. Higgins, B. L., Berry, D. W., Bartlett, S. D., Wiseman, H. M. & Pryde, G. J. Entanglement-free heisenberg-limited phase estimation. *Nature* **450**, 393–396 (2007).
26. Demkowicz-Dobrzanski, R. Multi-pass classical versus quantum strategies in lossy phase estimation. *Laser Phys.* **20**, 1197–1202 (2010).
27. Boixo, S., Flammia, S. T., Caves, S. T. & Geremia, J. M. Generalized limits for single-parameter quantum estimation. *Phys. Rev. Lett.* **98**, 090401 (2007).
28. Napolitano, M. *et al.* Interaction-based quantum metrology showing scaling beyond the Heisenberg limit. *Nature* **471**, 486–489 (2011).
29. Dorner, U. *et al.* Optimal quantum phase estimation. *Phys. Rev. Lett.* **102**, 040403 (2009).
30. Demkowicz-Dobrzanski, R. *et al.* Quantum phase estimation with lossy interferometers. *Phys. Rev. A* **80**, 013825 (2009).
31. Shaji, A. & Caves, C. M. Qubit metrology and decoherence. *Phys. Rev. A* **76**, 032111 (2007).
32. Andrè, A., Sorensen, A. S. & Lukin, M. D. Stability of atomic clocks based on entangled atoms. *Phys. Rev. Lett.* **92**, 230801 (2004).
33. Meiser, D. & Holland, M. J. Robustness of heisenberg-limited interferometry with balanced fock states. *New J. Phys.* **11**, 033002 (2009).
34. Zhengfeng, J., Guoming, W., Runyao, D., Yuan, F. & Mingsheng, Y. Parameter estimation of quantum channels. *IEEE Trans. Inf. Theory* **54**, 5172–5185 (2008).
35. Datta, A. *et al.* Quantum metrology with imperfect states and detectors. *Phys. Rev. A* **83**, 063836 (2011).
36. Kacprzycz, M., Demkowicz-Dobrzanski, R., Wasilewski, W., Banaszek, K. & Walmsley, I. A. Experimental quantum enhanced phase-estimation in the presence of loss. *Nat. Photon.* **4**, 357–360 (2010).
37. Thomas-Peter, N. *et al.* Real-world quantum sensors: evaluating resources for precision measurement. *Phys. Rev. Lett.* **107**, 113603 (2011).
38. Kolodyński, J. & Demkowicz-Dobrzanski, R. Phase estimation without *a priori* phase knowledge in the presence of loss. *Phys. Rev. A* **82**, 053804 (2010).
39. Knysh, S., Smelyanskiy, V. N. & Durkin, G. A. Scaling laws for precision in quantum interferometry and the bifurcation landscape of the optimal state. *Phys. Rev. A* **83**, 021804(R) (2011).
40. Escher, B. M., de Matos Filho, R. L. & Davidovich, L. General framework for estimating the ultimate precision limit in noisy quantum-enhanced metrology. *Nat. Phys.* **7**, 406–411 (2011).
41. Matsumoto, K. On metric of quantum channel spaces. Preprint at arxiv: 1006.0300 (2010).
42. Fujiwara, A. & Imai, H. A fibre bundle over manifolds of quantum channels and its application to quantum statistics. *J. Phys. A: Math. Theor.* **41**, 255304 (2008).
43. Bollinger, J. J., Itano, W. M., Wineland, D. J. & Heinzen, D. J. Optimal frequency measurements with maximally correlated states. *Phys. Rev. A* **54**, R4649–R4652 (1996).
44. Dowling, J. P. Correlated input-port, matter-wave interferometer: quantum-noise limits to the atom-laser gyroscope. *Phys. Rev. A* **57**, 4736–4746 (1998).
45. Bengtsson, I. & Zyczkowski, K. *Geometry of Quantum States: An Introduction to Quantum Entanglement* (Cambridge University Press, 2006).
46. Kay, S. M. *Fundamentals of Statistical Signal Processing: Estimation Theory*, Prentice Hall, 1993.
47. Nielsen, M. A. & Chuang, I. L. *Quantum Computing and Quantum Information* (Cambridge University Press, 2000).
48. Ruskai, M. B., Szarek, S. & Werner, E. An analysis of completely-positive trace-preserving maps on 2×2 matrices. *Lin. Alg. Appl.* **347**, 159–187 (2002).
49. Caves, C. M. Quantum-mechanical noise in an interferometer. *Phys. Rev. D* **23**, 1693–1708 (1981).
50. Pezze, L. & Smerzi, A. Mach-Zehnder interferometry at the Heisenberg limit with coherent and squeezed-vacuum light. *Phys. Rev. Lett.* **100**, 073601 (2008).
51. Genomi, M. G., Olivares, S. & Paris, M. G. A. Optical phase estimation in the presence of phase-diffusion. *Phys. Rev. Lett.* **106**, 153603 (2011).
52. Pinel, O. *et al.* Ultimate sensitivity of precision measurements with intense Gaussian quantum light: a multimodal approach. *Phys. Rev. A* **85**, 010101(R) (2012).
53. Jarzyna, M. & Demkowicz-Dobrzanski, R. Quantum interferometry with and without an external phase reference. *Phys. Rev. A* **85**, 011801(R) (2012).
54. Molmer, K. Optical coherence: a convenient fiction. *Phys. Rev. A* **55**, 3195 (1996).
55. Fujiwara, A. Quantum channel identification problem. *Phys. Rev. A* **63**, 042304 (2001).
56. Jamiolkowski, A. Linear transformations which preserve trace and positive semidefiniteness of operators. *Rep. Math. Phys.* **3**, 275–278 (1972).
57. Choi, M.- D. Completely positive linear maps on complex matrices. *Lin. Algebr. Appl.* **10**, 285–290 (1975).
58. Grant, M. & Boyd, S. CVX: Matlab software for disciplined convex programming, <http://cvxr.com/cvx/> (2011).

Acknowledgements

We thank Konrad Banaszek for many inspiring discussions and constant support. R.D.-D. and J.K. were supported by the European Commission under the IP project Q-ESSENCE, ERA-NET CHIST-ERA project QUASAR and the Foundation for Polish Science under the TEAM programme. M.G. was supported by the EPSRC Fellowship EP/E052290/1.

Author contributions

M.G. conceived the CS method. J.K. developed the CE method and utilized both approaches to obtain the exemplary analytic results. R.D.-D. proved the optimality of local tangent CS, the relation between the methods and formulated the semi-definite programming approach to CE. All authors contributed extensively to the manuscript with the leading input from R.D.-D.

Additional information

Supplementary Information accompanies this paper at <http://www.nature.com/naturecommunications>

Competing financial interests: The authors declare no competing financial interests.

Reprints and permission information is available online at <http://npg.nature.com/reprintsandpermissions/>

How to cite this article: Demkowicz-Dobrzański, R. *et al.* The elusive Heisenberg limit in quantum-enhanced metrology. *Nat. Commun.* 3:1063 doi: 10.1038/ncomms2067 (2012).

License: This work is licensed under a Creative Commons Attribution-NonCommercial-Share Alike 3.0 Unported License. To view a copy of this license, visit <http://creativecommons.org/licenses/by-nc-sa/3.0/>